

SCHOOL OF PHYSICS AND ASTRONOMY

YEAR 3 INTERIM PROJECT REPORT

SESSION 2018-2019

Name:	Hayley Barratt-Bentley
Student Number:	C1539373
Degree Programme:	BSc Physics with Astronomy
Project Title:	Optical observations of supernovae
Supervisor:	Dr. Paul Roche
Assessor	Dr. Sarah Ragan

Declaration:

I have read and understand Appendix 2 in the Student Handbook: "Some advice on the avoidance of plagiarism".

I hereby declare that the attached report is exclusively my own work, that no part of the work has previously been submitted for assessment (although do note that material in "Interim Report" may be re-used in the final "Project Report" as it is considered part of the same assessment), and that I have not knowingly allowed it to be copied by another person.

1 Abstract

This interim report presents an overview of supernovae research, a brief literature review and analysis of both new data sources and collections from the data archive. Analysis within this report has been performed through Astroimage J on sources: Gaia18dfy, Gaia18aen, Gaia18beg, Gaia16agf and ASAS-SN 15sf.

Contents

2	Introduction to supernovae	3
2.1	What are supernovae	4
2.2	What causes supernovae	5
2.3	History of observations	9
3	Data resources	10
3.1	Gaia	10
3.2	ASAS-SN	12
4	Methodology	13
4.1	Introduction to the Las Cumbres Observatory network	13
4.2	FITS format data	15
4.3	Data analysis using Astroimage J	16
4.4	Gaia Alerts and observations through LCO	20
5	Data analysis	22
5.1	Image processing post data collection	22
5.2	Data collection from LCO	23
5.3	Data analysis from LCO science archive	26
6	Error analysis	29
6.1	Numerical error analysis	29
6.2	Photometry errors	29
7	Future work	31
7.1	Data collection and analysis	31
7.2	Development of type Ia supernovae	31
	Bibliografia	32

2 Introduction to supernovae

This chapter is to inform on what supernovae are, what causes them, the different types which form in the universe and the history of observations dating back to 185AD[2]. A constantly developing field enables research into predictions on how the universe began, but also, how It may end. This research, especially into that of type Ia stars, enables the development of the age of the Universe and also significantly aids the field of dark energy.

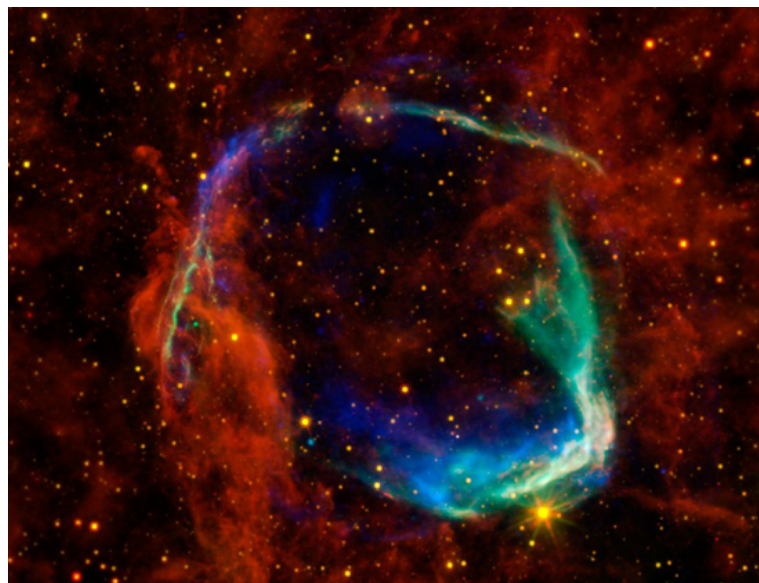


Figure 1: WISE image of SN 185[3]

2.1 What are supernovae

Death of low-mass stars, initial masses < 11 solar masses, end their lives by exhausting their hydrogen core and then evolve off of the main sequence into stars such as a red giant stars or as white dwarfs[6]. However, stars of a higher stellar mass form supergiant stars. These evolve rapidly to form a layered structure of concentric zones of nuclear burning around the core, where eventually conditions in the core allow silicon burning to take place and form iron group elements.

As these reactions slow to a stop, the core must contract under gravity and the temperature and density continue to increase but no longer with nuclear reactions to release energy to balance the force of gravity. This imbalance causes core collapse which is the most frequent form of supernovae explosions, found in star-forming regions where young, massive stars are found[5].

2.2 What causes supernovae

2.2.1 Type II supernovae

As aforementioned these are caused by core collapse and are associated with massive, young stars which evolve rapidly into supernovae[7]. Type II supernovae candidates progress through the main sequence and leave to form massive red super giants, forming the layered structure previously mentioned beginning to fuse iron. This causes an iron build up to occur in their core which causes them to reach the Chandrasekhar Mass[9]:

$$M = \left[\frac{1}{4\pi G_N^3} \frac{P_c^3}{\rho_c^4} \right]^{\frac{1}{2}} \varphi_3 = \frac{\sqrt{3}\pi}{16} \left(\frac{1}{G_N^3 m_N^4 \mu_e^4} \right)^{\frac{1}{2}} \varphi_3 = 1.46 \left(\frac{2}{\mu_e} \right)^2 M_{\odot} \equiv M_{Ch}$$

Figure 2: Chandrasekhar mass equation

The Chandrasekhar mass is used to calculate the mass of white dwarfs or in this case degenerate core of evolving stars[11]. Iron cores are supported by electron degeneracy pressure, as nuclear fusion in the shells surrounding the core continue to add mass, it reaches the Chandrasekhar limit causing a rapid gravitational collapse [11].

The time in which It takes a star to collapse is shown by the equation below:

$$t_{dyn} \approx \left(\frac{2r^3}{GM_r} \right)^{0.5} \approx \frac{1}{(G\rho)^{0.5}}$$

Figure 3: Time for stellar collapse equation

Post collapse this forms a neutron star and expels an envelope, some of which falls back onto the neutron star, this neutron star is then referred to as the supernovae remnant and if exceeding the limiting mass of a neutron star (Core mass <3 solar masses), would form a black hole.

2.2.2 Type I supernovae

Type Ia are from mergers in white dwarf binary systems, these accrete mass from a companion star and eventually reach Chandrasekhar mass[9]. High temperatures cause ignition of nuclear burning reactions, causing the star to explode. Unlike type II supernovae, this leaves no remnant.

These supernovae are classified from characteristic light curves and absorption of Silicon in their emission spectra at 6150 Angstroms. After the explosion, B-magnitudes decline gradually across the first 15 days, when peak luminosity occurs [12]. Peak /maximum luminosity is used to determine the distance from observer to observed supernovae. More on this distance calculation, using a type I supernova as a standard candle, will be discussed later in the report in project progression.

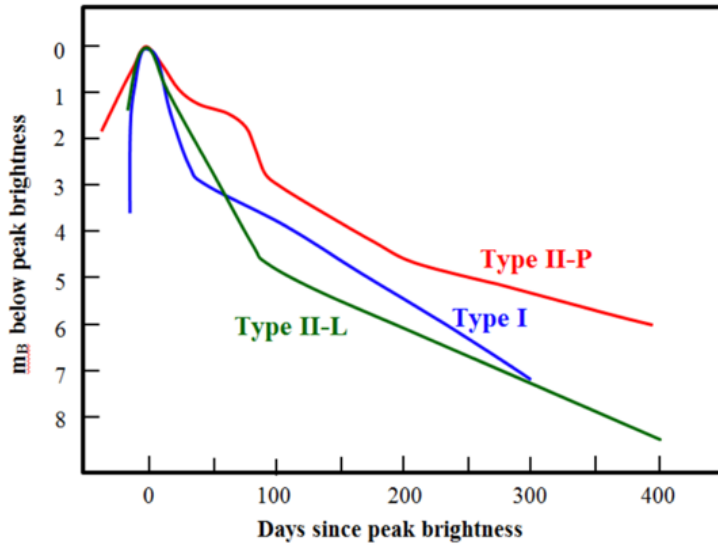


Figure 4: Characteristic light curve plot [13]

Similarly to type I classification, distinction between type Ia and type Ib supernovae is found by distinguishing through spectral observations. Type Ib supernovae have spectral absence of silicon features visible in type Ia spectra. They are also both found in star-forming regions, often in the arms of spiral galaxies close to HII regions [14].

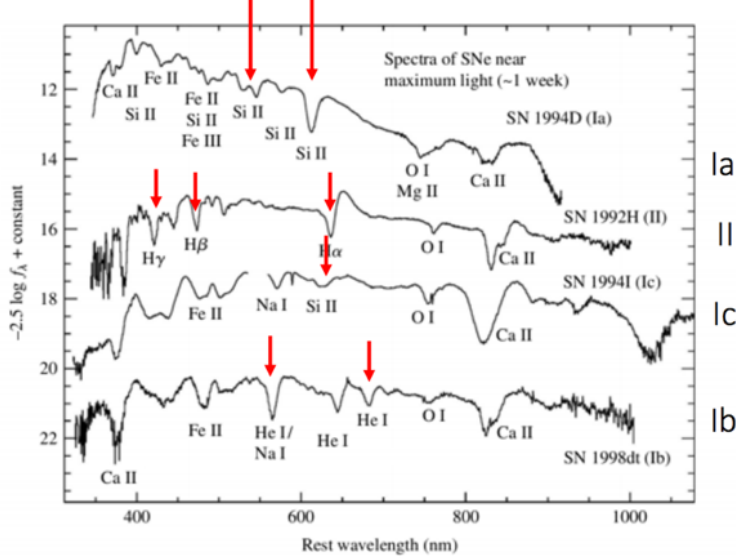


Figure 5: Emission spectra plot showing types of supernovae [14]

As type Ib are a result of core-collapse of massive stars, the largest difference between them and type II is the progenitor loses its outer layer of hydrogen prior to the core collapse and then type 1c are similar in that they lose both their hydrogen and helium layers prior. This leaves the Ib spectra with no Silicon but a Helium emission line and the Ic spectra with neither[15].

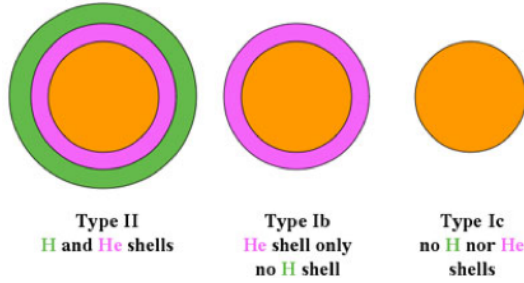


Figure 6: Plot showing stellar layers before collapse [16]

2.2.3 Classification of supernovae

As previously mentioned the distinguishable factor which classifies the majority of supernovae is that of the presence or absence of particular features in their optical spectra taken near the time of peak luminosity. This divides them into their 4 types and thus their naming convention.

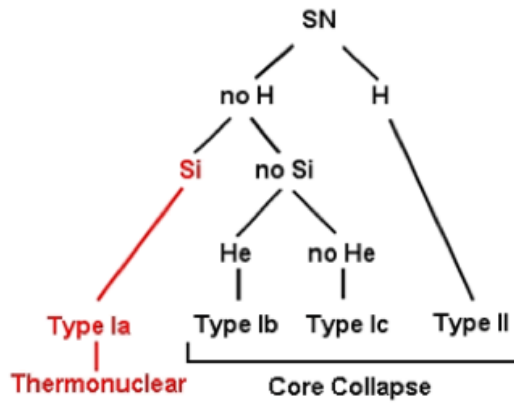


Figure 7: Naming classification of supernovae [17]

2.3 History of observations

Supernovae, first observed by Chinese astronomers in 185 AD. The first confirmed identification of a supernovae was identified by its radio supernovae remnant[18], a supernovae remnant being when a fraction of stellar mass is ejected, often sweeping up surrounding material and possibly colliding with neighbouring molecular clouds[19].

It is the slow-moving shell, often referred to as the ‘snowplow phase’ of the remnant, which with its slow-moving outer shock and hot interior emits X-rays long after the event occurs, enabling the later confirmation of the 393 AD observation [?]. Radio supernovae are quite rare as the ability to observe them is heavily limited by the sensitivity of radio arrays and most detected this way are associated with Type II supernovae[21].

Observation astronomy was very different prior to the invention of the telescope in 1608 by German-Dutch lens-maker Hans Lippershey and then first applied to observations by Galileo Galilei in 1609[22]. Prior, supernovae were observed by the naked eye. When a star was too dim to be observed with the naked eye but then suddenly flared, observers would refer to these as new stars, since new in Latin is the word ‘nova’ this is where the name came from.

Although no observation of supernovae has been made since the invention of the telescope, in our galaxy, it is thought this is due to stellar dust from previous explosions blocking light from such events[23].

3 Data resources

3.1 Gaia

Gaia Science Alerts program, launched in December 2013, mission's purpose was to observe more than 1×10^9 stars in the Milky Way, also enabling transient objects to be observed[24]. The team working on this project is that of: Cambridge and Warsaw astronomy research groups, this team works on rapid response analysis of daily Gaia data deliveries. Averaging about 50×10^6 observations per day, their task involves identifying and characterising anomalous or astrophysical sources.

The data collected on transient observations and that of events such as supernovae require lots of follow up observations due to the short-lived nature of the events. By setting up the Gaia alerts program it enables additional follow-up observations to be made using the LCO network by astronomers throughout the world. Across their 5 year mission it is expected that around 6000 supernovae, down to approximately 19 magnitude will be observed.

3.1.1 How the detection system works

Gaia's satellite has on-board a 1 Gigapixel camera which is able to scan the sky and determine the position and brightness of each source. Taking 45 seconds to observe across the whole focal plane, observations of the same area in the sky will usually occur after around 30 days of the first observation. Follow up of each source provides more detailed information and classification of the discovered sources[24].

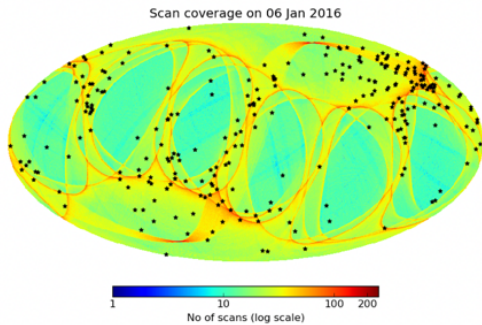


Figure 8: Sky scan coverage in 2016

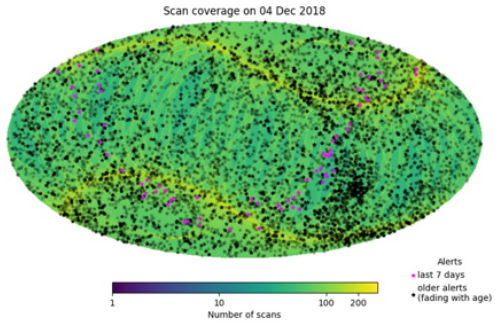


Figure 9: Sky scan coverage in 2018

Given data collection can detect thousands of observations each day, the alerts team reduce this data using the developed AlertPipe software. This software, run in the Institute of Astronomy, Cambridge, puts a new source alert through a system to compare that to the same observation at that location previously taken, to monitor any variation in magnitude of said source. When there is a significant fluctuation the source is then analysed using available Gaia data to try to determine what the observation is of. The flow chart below shows how the determination of where the transient lies takes place.

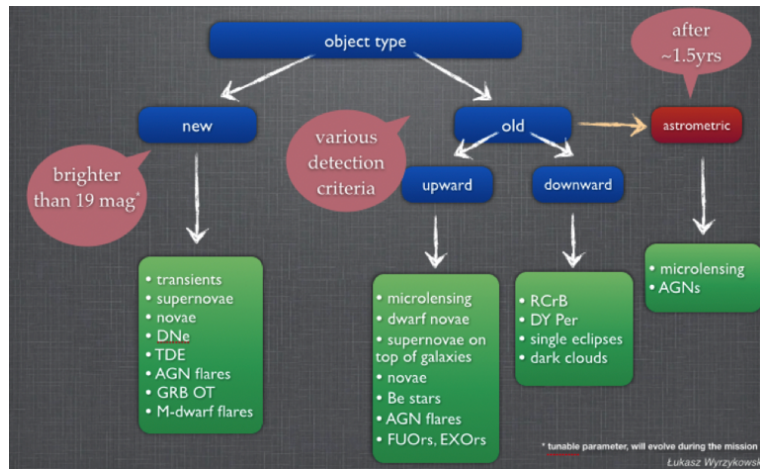


Figure 10: Flow chart of Gaia pipeline [27]

3.2 ASAS-SN

ASAS-SN are the All-Sky Automated survey for Supernovae, funded by the Gordon and Betty MOORE foundation and hosted by LCO, they are a network similar to Gaia and will be presented more in-depth in following research.

4 Methodology

This chapter covers the data analysis techniques used to produce light curves of supernovae from data obtained on the LCO network. It will introduce the network, discuss the image data format and include a step-by-step guide to data collection and analysis.

4.1 Introduction to the Las Cumbres Observatory network

The Las Cumbres Observatory (LCO) global science network observes and researches throughout many areas of astronomy, e.g. Exoplanets, NEOs and Supernovae. [8] The scope of the network allows the observation of objects which need to be monitored for long periods but also transients which appear suddenly without warning. Being an integral partner in many supernovae surveys, have developed the field significantly[29]. The two collaborative projects which impact on this particular work are

ASAS-SN

and

Gaia.

LCO: The key initiative is the Supernova Key Project which aims to build the world's largest sample of data on local supernovae by observing 500 supernovae in 3 years[30]. This was already achieved within 2 years when they had provided $>80,000$ images and 2,000 spectra. Currently they monitor 30-40 active supernovae and such rapid response projects allow the community to obtain fast classification of the events. To see more on this project visit: <http://adsabs.harvard.edu/abs/2017AAS...22934110H>

The LCO network accessible with this project consists of 5 image telescopes, 2 spectrographs and multiple filters as listed below:

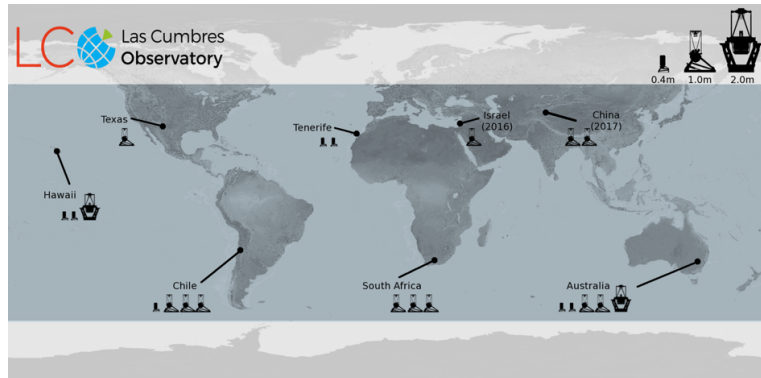


Figure 11: LCO telescope network map[31]

Type	Name	Class	Pixel scale	Field of view	Filter wheel options
Imager	Spectral	2-meter	0.300 (bin 2x2)	10'x10'	18
	Sinistro	1-meter	0.389 (bin 1x1)	26'x26'	21
	SBIG 6303	0.4-meter	0.571 (bin 1x1)	29'x19'	9
	Merope	2-meter	0.278 (bin 2x2)	5'x5'	18
	SBIG	1-meter	0.464 (bin 2x2)	15.6'x15.8'	21
Type	Name	Class	Wavelength coverage /nm	Resolution	Nm per pixel
Spectrographs	FLOYDS	2-meter	540-1000 / 320-570	400-700	0.35-0.17
	NRES	1-meter	380-860	6x 53000	---

Figure 12: LCO telescope table [32]

To find out more about the filters deployed with each telescope further information is on <https://lco.global/observatory/filters/>

4.2 FITS format data

Data collected from the LCO network can be downloaded from the portal in the format of a FITS file. FITS file (Flexible Image Transport System) files are an open standard, defining a digital file format making it useful for storage, transmission and processing of data[33].

4.3 Data analysis using Astroimage J

This section will be a brief methodology for how to use Astroimage J to produce light curve data from .fits image files.

1. Ensuring images are fits files, import into astroimage J. Select option “Use virtual stack” to keep all images together and “Sort names numerically” to ensure images would remain in correct order.
2. Images need sorting through, eliminating any blurry or flared image and editing exposure ensuring to “display as image negative” making objects easier to resolve, see figure.

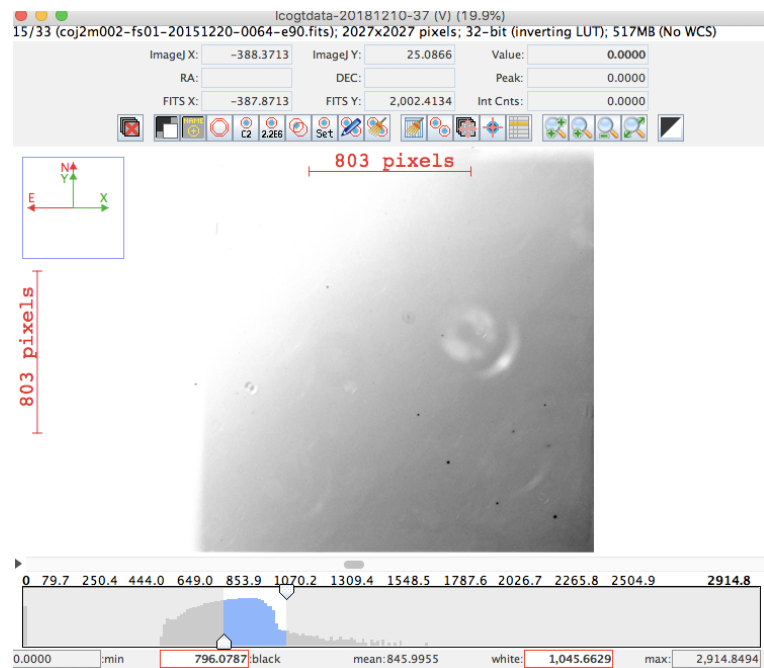


Figure 13: Exemplar image to be discarded due to exposure

3. Images required to be rotated to correct orientation using comparison images from different sources and if not already north facing view, invert Y.

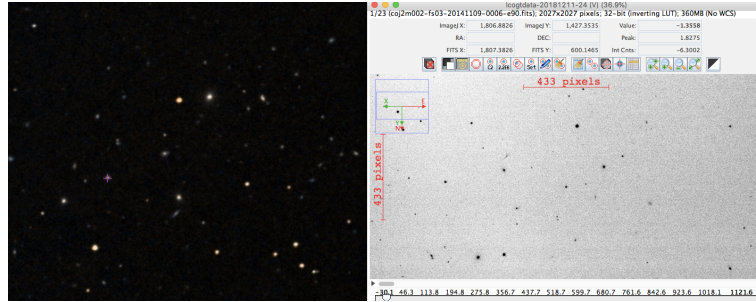


Figure 14: Exemplar image of Gaia alerts data for orientation comparison

4. Brightness and contrast adjustments can be made using bottom scroll bar to get a clearer image, increasing clarity of objects.
5. Observations across multiple different frames are used in order to see a fluctuation of magnitude, any variability measured in the image needed to be analysed. This is to ensure correct variability is measured and is not caused by other factors
6. Ensure to establish multiple comparison stars to ensure correct variability of supernovae observed and evaluate ones which are clear in every image and non-elliptical (more likely to vary themselves). As many suitable variable stars should be chosen and used in the photometry.
7. Aperture radius is determined by area in the image for which the pixels for observed object lay within. Use the straight line tool to draw over the target object horizontally.

8. The Analyse function is used to plot a seeing profile shown below and three values in red on the bottom of the window need to be noted for further photometry.

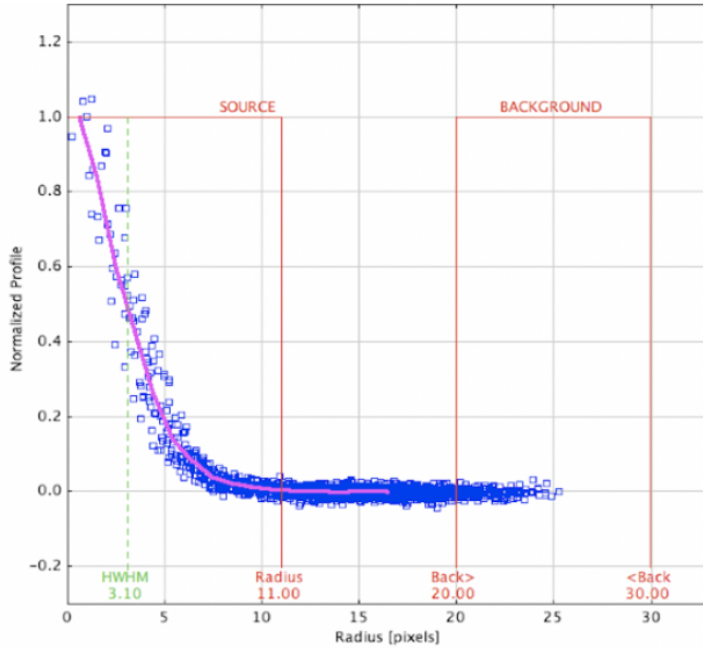


Figure 15: Exemplar image of seeing profile plot from AstroimageJ

9. Multiple aperture function is used, ensuring it is on single step mode, is not using previous apertures and that numbers from the last figure are inputted into: “Radius of object aperture”, “Inner radius of background annulus” and “outer radius of background annulus”, when correct place apertures.
10. Select the main target and follow by selecting comparison stars and finally the enter key. Once all images are analysed save data to a new file.
11. Magnitude can be calculated within said file in excel. Calculated by using ‘rel flux T1’ column the function =2.5*log10 (“Data column number”).

12. Plot Julian Date with magnitude putting the y-axis reversed and minimums set to focus on the data.

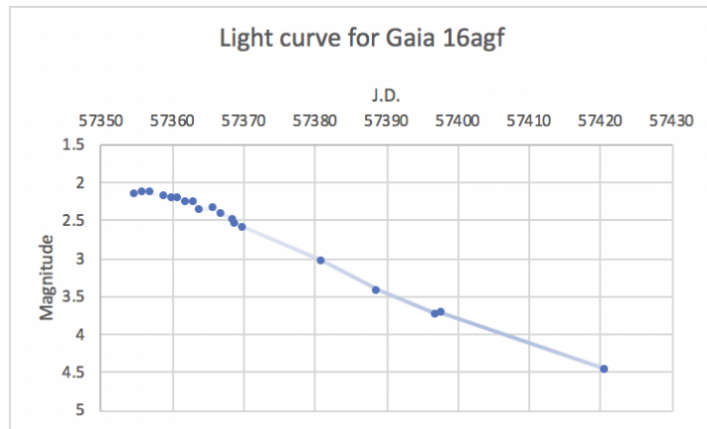


Figure 16: Exemplar light curve plot of Gaia 16agf

4.4 Gaia Alerts and observations through LCO

Gaia alerts index is used to find suitable sources to be observed. Key features that are looked for on the alerts index are the following:

4.4.1 Acting on alerts

- **Appropriate magnitudes:** 12-16 magnitudes for 1m telescopes, 16-19 for 2m telescopes, no lower than 19. To observe good supernovae light curves, observations need to be made on the initial climb, capturing the peak and watching the magnitudes descent following weeks/months.
- **Historic magnitude:** A useful indicator of how much the object's magnitude has risen and thus showing if it is likely to be a supernova depending on increase in magnitude. A substantial increase in magnitude, but not such an increase miss peak magnitude, is that of 0.5-1 magnitude.
- **Recent observation date:** Observations which cause the alert need to be within the last 48 hours for it to be feasible to capture the beginning of the light curve, initial increase often occurs within 7-14 days.
- **Minimum candidate supernovae:** Within the comment section of the Gaia alerts index there will often be a statement of what the alert is predicted or clarified to be. Within this section the aim is to find candidate or confirmed supernovae.
- **Observability:** Needing to be performed outside the Gaia alerts index, instead using StarALT. The RA and DEC from the observation would be input in along with the location of the telescope proposed to observe from (depending on whether 2,1 or 0.5 m are needed, a larger issue for the 2m). This will then enable visibility to be tracked for the duration of the observation, informing if tracking the object for the next few months and gain a sufficient amount of data is possible.

4.4.2 Using the LCO observation portal

On the LCO observing portal it has lots of resources, aiding the construction of requests. This methodology will be included in the next report.

5 Data analysis

This chapter illustrates the analysis performed on collected data from the LCO network and from the archive data respectively, presenting errors generated within photometry and LCO data on figure plots.

5.1 Image processing post data collection

5.1.1 Funpack

From the submitted observation requests window once an observation has completed, data can be downloaded in the form of a fits.fz file. To analyse this the file needs to be converted, using the terminal (for Mac OS) and the Funpack package, into an average fits file enabling it to be used within AstroimageJ. For Mac OS, once funpack has been downloaded the following should be inputted into the terminal and convert files to .fits format.

```
cd  
cd documents  
cd (folder name containing fits.fz files)  
for image in *  
do  
funpack -F DOLLARimage  
done.
```

5.2 Data collection from LCO

Observation requests have been made using the LCO portal for this project since November 10th and since then the following objects have been observed in order of observation date[34]:

- Gaia 18dfy
- Gaia 16djh
- Gaia 18dkc
- Gaia 18dru

The following will outline the success of each observation and information on the object observed and why it was chosen.

5.2.1 Gaia 18dfy

The observation requested for Gaia18dfy was submitted on 2nd of November and it was a relatively successful first observation. Initially it was observed on the 2.0-meter spectral telescope, using both B and V filters for an exposure of 30 seconds. This output 4 out of 6 observations as successful across 6 days, obtaining 8 images of the object. A second request to follow this observation requested for the 8th of November with an edited exposure time of 60 seconds, to enable better clarity of the object given its low magnitude. With this new submission however, only 2 out of 5 observations were successful, ending in 10 total images of the object in 2 filters across 5 time steps.

Data was then analysed in AstroimageJ and a graph was plotted including both filters as shown below, blue and red representing the B and V filter respectively.

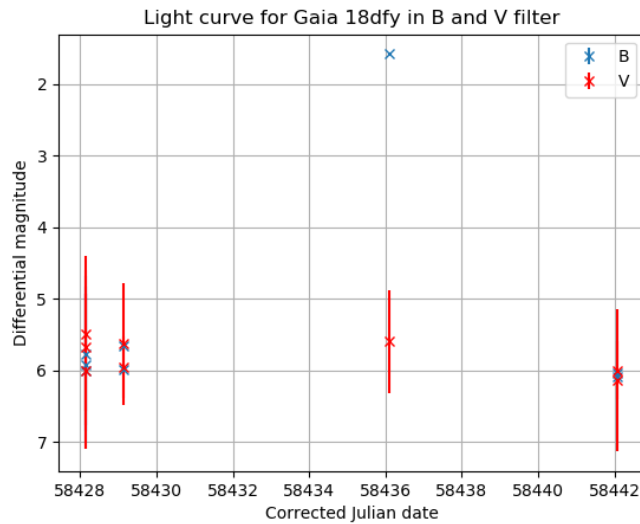


Figure 17: Graph of B and V magnitude data sets

From this graph due to the final 2 points being made at a different exposure and the plot being of differential magnitude to comparison stars rather than absolute magnitudes, data shows no clear light curve. This is unfortunately due to multiple of the observation windows timing out leaving less data to work with. Due to this particular object being one of a relatively high magnitude and the error margins being so substantial, there is no sufficient evidence of a significant magnitude change, therefore, it was decided to instead request to observe some objects of lower magnitude.

The follow up section for this object has been updated using data collected on the source and presented on the Gaia index page. As this uses absolute magnitudes it shows a much clearer drop in magnitude from the alerting magnitude give above.

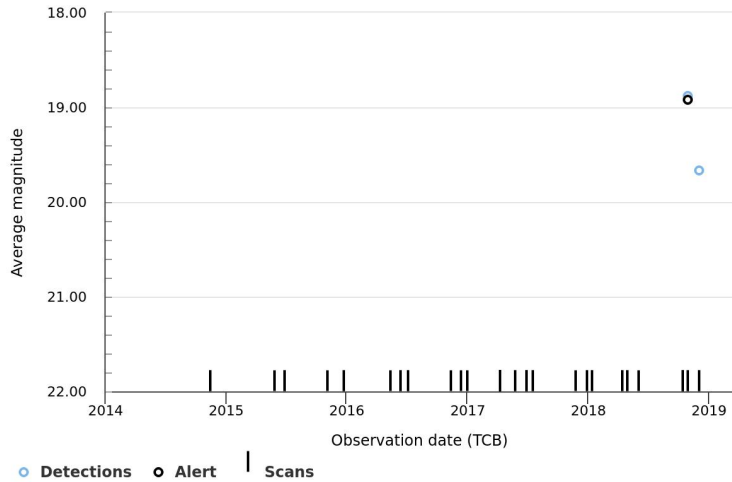


Figure 18: Absolute magnitude plot of Gaia 18dfy from [34]

5.2.2 Other observations

Unfortunately, regarding the other observations put in for this project, two were unable to obtain any data due to observation windows not being available and the other source went below a magnitude of 19, rendering the equipment available unsuitable even with longer exposures.

5.3 Data analysis from LCO science archive

In order to produce more suitable light curves and develop analysis skills on supernovae light curves, data was used from the LCO science archive. Objects chosen for observation were chosen using the Gaia alerts search function to determine recent type Ia supernovae which had been observed and then filtered down regarding whether or not they had obtained sufficient data through LCO observations. Objects analysed were as follows:

- Gaia 18beg
- Gaia 18aen
- ASAS-SN 15sf
- Gaia 16agf

Below presents light curves generated from archive data across the 4 targets analysed.

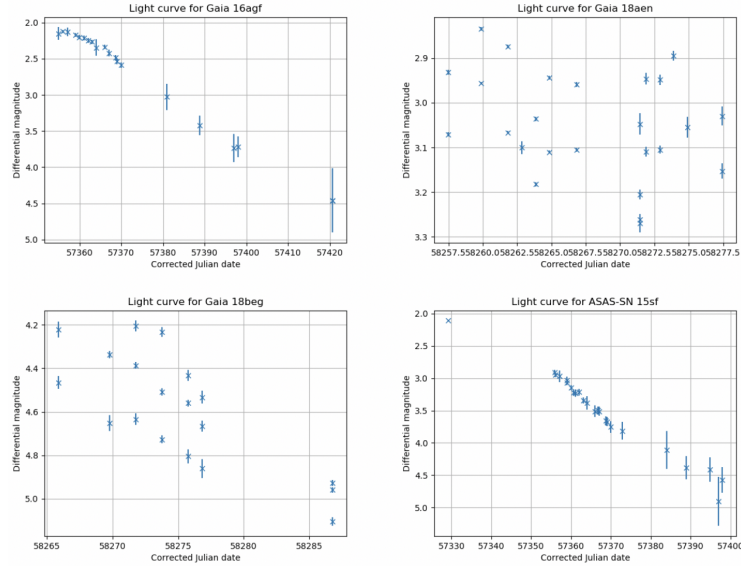


Figure 19: Archive light curve plots of various transients

5.3.1 Classification of archive data targets

To best represent a wide dataset of transients, analysis was done of two type Ia supernovae, one super-luminous supernovae (SLSN) and one unknown transient. From

Target	RA - DEC	Class
Gaia 16agf	98.53741-25.18462	SN Ia
Gaia 18aen	120.71694-30.31032	Unknown
Gaia 18beg	165.62621-55.59883	SLSN
ASAS-SN 15sf	2.86509-6.4273	SN Ia

Figure 20: Archive key data for various transients

the graphs formed it shows the way in which type Ia supernovae can be detected by their characteristic light curves, given it is supported by a good data set. The SLSN plot has a distinctive decline in magnitude; however, fluctuation in magnitude is not smooth. This is likely related to the distance in which it is being observed from and the nature of its surroundings (lack of comparison stars).

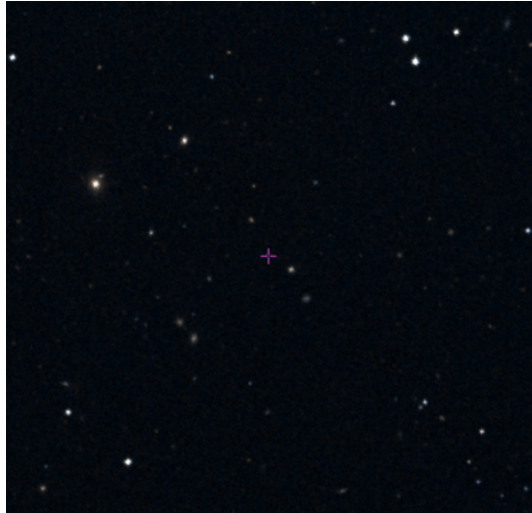


Figure 21: Astronomical image of Gaia 18beg

Comparably Gaia16agf generates a very clean plot showing a peak and steady magnitude decline and as visible in the figure below, it has considerably more comparison stars, resulting in a better evaluation of differential magnitude.

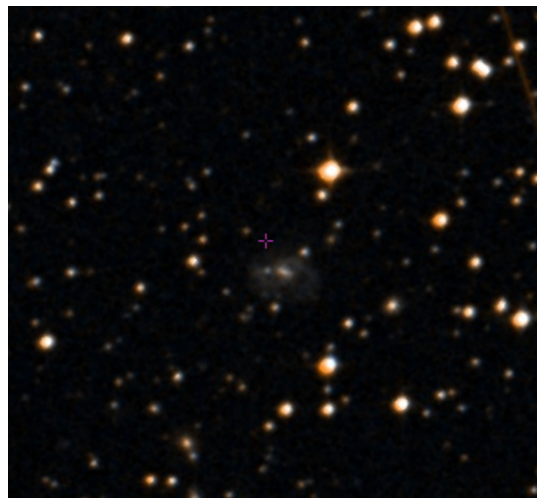


Figure 22: Astronomical image of Gaia 16agf

..

6 Error analysis

This chapter will cover a brief overview of data analysis used within this report, this will go much deeper come the final report.

6.1 Numerical error analysis

Within evaluating figures () error bars were generated from the output differential magnitude errors given by Astroimage J. These errors, given in flux, were converted to mag with the following equation[35].

$$\Delta \log_b(x) \approx \frac{\Delta x}{x \cdot \ln(b)}$$

Figure 23: Where b=base of the log, deltax= error in flux and x output flux.

This generated error bars for the y-axis plotted on project graphs in this report, as a function of:

$$\text{Magnitude error} = 2.5 \times \left(\frac{\text{flux error}}{2.3 \times \text{flux}} \right)$$

Figure 24: Error equation for flux, same used to determine flux is methodology.

6.2 Photometry errors

Two common ways to analyse datasets in photometry is through the signal to noise ratio (SNR) or using the standard deviation for comparison stars. The preferred method over the two is that of using comparison stars. This provides a simple measure of uncertainty by taking the standard deviation of a series of comparison star measurements and calculates an average deviation from the mean[36].

Being the comparison stars determined in the methodology for this method, I believe most of the data is preproduced from the Astroimage J data file created. Astroimage J also outputs an error flux for each star measured which, using this method, will be a stronger error analysis than purely using error generated for the flux of the variable star measurement; however, for data collected within this report the datasets were not large enough to form an error representing this method.

$$\sigma_{K-C} = \sqrt{\frac{1}{n-1} \sum (x - \bar{x})^2}$$

Figure 25: Error where K and C are key target and comparisons respectively

$$Dq = \sqrt{\sigma^2 K - C + \left(\frac{1}{SNR}\right)^2}$$

Figure 26: Error equation photometry utilising comparison stars and SNR.

With bigger datasets the equation below, adding in the uncertainty over all time series and from the SNR is much more suitable.

This equation accounts for durations of low SNR, which often occur due to intervals of tracking hindered by weather conditions, also covering for fluctuations in magnitude of comparison stars.

7 Future work

7.1 Data collection and analysis

Plans for continuing this work are largely based around obtaining larger data sets and developing errors to best represent the errors laying within both the software used and the photometry itself.

A way which is planned to increase the worth of data sets obtained is through conversions to absolute magnitudes. From figure 18 you can see a Gaia portal follow up graph which contain absolute magnitude measurements. Once data sets have been obtained, higher levels of analysis will be used to determine the absolute magnitudes of the source in collected images. This does not only make for better comparisons to the sources state prior to fluctuation but will also enable the project to rule out objects which fluctuate too much or too little to be the supernovae type wanting to be researched.

7.2 Development of type Ia supernovae

A further use for converting to absolute magnitudes is that of developing data of type Ia supernovae to follow the magnitude of standard candles and thus find a value for Hubble's constant/ the age of the universe. From calculating this, it will not only develop data analysis but also help determine the validity of collected results.

References

- [1] Adam G. Riess, Louis-Gregory Strolger, John Tonry, Stefano Casertano, Henry C. Ferguson, Bahram Mobasher, Peter Challis, Alexei V. Filippenko, Saurabh Jha, Weidong Li (2004—) *Type Ia Supernova Discoveries at $z \geq 1$ from the Hubble Space Telescope: Evidence for Past Deceleration and Constraints on Dark Energy Evolution* The Astrophysical Journal, Volume 607, Number 2.
- [2] Richard G. Strom (1994) *SN 185, its associated remnant and PSR 1509* Monthly Notices of the Royal Astronomical Society, Volume 268, Issue 1, pages L5-L9.
- [3] N/A (2016) *Figure of supernovae sn185* <https://www.space.com/13374-ancient-supernova-mystery-solved.html>, Accessed: (December 2018)
- [4] Patrick L. Kelly, Alexei V. Filippenko, David L. Burke, Malcom Hicken, Mohan Ganeshalingam (2015) *Distances with 14 percent precision from type Ia supernovae in young star-forming environments* Science Journal, Volume 347, Issue 6229, pages 1459-1462
- [5] Tim Lichtenberg Richard J. Parker Michael R. Meyer (2016) *Isotopic enrichment of forming planetary systems from supernova pollution* Monthly Notices of the Royal Astronomical Society, Volume 462, Issue 4, 11 November 2016, Pages 3979–3992
- [6] Open university textbook REF
- [7] S. Valenti, D. A. Howell, et. al (2016)
The diversity of Type II supernova versus the similarity in their progenitors Monthly notices of the Royal Astronomical Society, Volume 459, pages 3939-3962
- [8] Simon F. Green, Mark H. Jones *An introduction to the Sun and Stars* Cambridge Open University
- [9] Nomoto, Ken'ichi, Leung, Shing-Chi (2017)
Thermonuclear Explosions of Chandrasekhar Mass White Dwarfs Handbook of Supernovae, ISBN 978-3-319-21845-8
- [10] DIPANKAR BHATTACHARYA, (2011)
Beyond the Chandrasekhar limit: Structure and formation of compact stars Pramana, Journal of Physics, Volume 77, No. 1

- [11] S.Valenti, D.A Howell, et. al (2016)
The diversity of type II supernovae versus the similarity in their progenitors
Monthly Notices of the Royal Astronomical Society, issue 459, pages 3939-3962
- [12] Paulo A. Mazzali, Friedrich K. Ropke, et. al (2007)
A Common Explosion Mechanism for Type Ia Supernovae Science Mag, volume 315, page 825-827
- [13] Bradley Carroll, Date Ostlie
Introduction to Modern Astrophysics Chapter 15, figure 7.
- [14] Bradley Carroll, Date Ostlie
Introduction to Modern Astrophysics Chapter 15.
- [15] Paulo A. Mazzali, Friedrich K. Ropke, et. al (2007)
A Common Explosion Mechanism for Type Ia Supernovae Science Mag, volume 315, page 825-827
- [16] N/A (2015)
Type Ic Supernovae, COSMOS <http://astronomy.swin.edu.au/cosmos/T/Type+Ic+Supernova>,
accessed: (September 2018).
- [17] N/A (2015)
Supernovae Classification, COSMOS <http://astronomy.swin.edu.au/cosmos/S/TSupernova+Classification>
Accessed: (September 2018).
- [18] Clark D.H, Stephenson F.R (1997)
Historical Supernovae New York, Pergamon Press
- [19] Olivier Ifrig, Patrick Hennebelle *Mutual influence of supernovae and molecular clouds*
- [20] D. A. Leahy, S. Ranasinghe (2012) *Radio observations of CTB80: detection of the snowplough in an old supernova remnant* Monthly Notices of the Royal Astronomical Society, Volume 423, pages 718-724
- [21] Nayana A.J, Chandra Poonam (2017) *GMRT radio detection of a type II supernova SN 2017eaw* The Astronomers Telegram, Issue 10534

- [22] NA (2018) *NASA- Telescope history* <https://www.nasa.gov/audience/forstudents/9-12/features/telescopefeature912.html>, Accessed: (October 2018)
- [23] NA (2018) *Supernovae Observations, Astronomy* <https://courses.lumenlearning.com/astronomy/chapter/supernova-observations/>, Accessed: (October 2018).
- [24] Lukasz Wyrzykowski (2014) *First year of Gaia Science Alerts* Cornell University Library publication
- [25] Lukasz Wyrzykowski (2014) *First year of Gaia Science Alerts* Cornell University Library publication, figure 2
- [26] NA (2018) *Gaia Alerts* <https://www.ast.cam.ac.uk/~ebreedt/GaiaAlerts.html>, Accessed: (December 2018)
- [27] Lukasz Wyrzykowski (2014) *First year of Gaia Science Alerts* Cornell University Library publication, figure 1
- [28] N/A (2018) *ASAS-SN* <http://www.astronomy.ohio-state.edu/~assassin/index.shtml>
- [29] N/A (2018) *LCO Observation Portal* <https://observe.lco.global>, Accessed : (December 2018).
- [30] Howell, Dale Andrew (2016) *The Supernovae Key Project* American Astronomical Society, ASS Meeting 229
- [31] Yannis Tsapras (2017) *Microlensing Key Project* <https://robonet.lco.global/research/>, Accessed: (November 2018)
- [32] N/a (2018) *Instruments, Las Cumbres Observatory* <https://lco.global/observatory/instruments/>, Accessed: (November 2018)
- [33] N/A (2018) *FITS Documentation Page* <https://fits.gsfc.nasa.gov/fitsdocumentation.html>, Accessed: (November 2018)
- [34] Cambridge University *Gaia Alerts Index* <http://gsaweb.ast.cam.ac.uk/alerts/alertsindex>, Accessed: (September-December 2018)
- [35] N/A (2016) *Propagation of Logarithms* <http://phys114115lab.capuphysics.ca/>, Accessed: (December 2018)

- [36] Koppelman M (2005) *Uncertainty Analysis in Photometric Observations* The Society for Astronomical Sciences, 24th Annual Symposium on Telescope Science. page 10